IET Renewable Power Generation

Research Article

Enhancing smart grid transient performance using storage device-based MPC controller

ISSN 1752-1416
Received on 22nd November 2016
Revised 9th May 2017
Accepted on 1st June 2017
E-First on 22nd June 2017
doi: 10.1049/iet-rpg.2016.0892
www.ietdl.org

Yara A. Sultan[1] ✉, Sahar S. Kaddah[1], Mostafa A. Elhosseini[2]
[1]Department of Electrical Engineering, Faculty of Engineering, Mansoura University, Mansoura, Egypt
[2]Department of Computers Engineering & Control Systems, Faculty of Engineering, Mansoura University, Mansoura, Egypt
✉ *E-mail: yaraabdalla2@gmail.com*

Abstract: Renewable energy sources (wind turbine and photovoltaic system) are connected to the smart grid to promote the grid power, but the output of these sources is changed due to the sunlight and wind speed variations. Power storage system has the ability to reduce variations in a power system. Battery energy storage system (BESS) and superconducting magnetic energy storage system (SMES) are good solutions for this problem. The storage unit is connected to a power system at the point of common coupling and is able to absorb/store both active and reactive powers from this system and inject them into the power system in the peak demand periods. A control strategy based on proportional–integrative–derivative (PID) and model predictive controller (MPC) are used to control (SMES/BESS) to enhance the transient performance of a smart grid. The proposed algorithm has been tested on standard IEEE 5-bus system connected to wind turbine distributed generator, non-linear loads, and storage device (BESS/SMES) to verify the superiority of the presented method. The simulation results show that the performance of SMES with PID is more efficient than BESS with PID, but they have nearly the same output when MPC control strategy is used.

1 Introduction

Smart grid is a power system integrated with renewable power sources such as wind turbine and photovoltaic that share their outputs with the grid with high penetration level production. Furthermore, it reduces carbon dioxide emissions and other pollutants [1].

Renewable sources are affected by natural conditions such as wind speed in wind turbine system and solar radiation in a photovoltaic system which means that it cannot provide continuous and stable output power. So, the distributed generator (DG) is usually incorporated into the electric power system at the distribution networks side to increase system stability and balance the amplitude of phase grid voltage.

Energy storage could be a solution to enhance system stability by storing/injecting energy according to system needs. Energy storage systems [2] have different concepts and can be mainly divided into two groups: the first group stores large amounts of energy, though it does not react so fast such as pumped hydrostorage (PHS). The second group stores smaller amounts of energy with a fast acting behaviour such as superconducting magnetic energy storage system (SMES) [3].

SMES-based voltage-source converter (VSC) improves transient as well as the dynamic stability of power system [4]. On the other hand, battery energy storage systems (BESSs) [5] are considered as the most common energy storage systems with renewable energy sources. BESS is a viable solution for small-scale renewable energy connected with smart grid due to its high-energy density. It uses electrochemical reactions to produce electricity at a fixed voltage. The energy is stored in the form of electrochemical energy in a set of multiple cells connected in series or parallel in order to achieve the desired electrical characteristics.

In the industry, most of the controllers are mainly proportional–integrative–derivative (PID) due to their cheap price and easy tuning. The PID controller solves most of the mono-variable control tasks. However, in multi-constrained systems, the controller does not always give satisfactory results. The model predictive controller (MPC) is a technique that focuses on constructing controllers that can adjust the control action before a change in the output set point actually occurs. MPC is a control strategy based on numerical optimisation at each interval, a future control input and future plant output are predicted and optimised using the MPC model. MPC control works based on a receding horizon policy that means the internal model predicts plant behaviour over a future horizon in time. MPC enables controllers to make adjustments that are smoother and closer to optimal control action value. The MPC is applied to SMES unit to control both dc–dc chopper and VSC in order to reduce any distortion or harmonics in the grid. Furthermore, the MPC is applied to control BESS [6].

The main contribution of this paper is to propose a new MPC controller for storage device SMES/BESS to overcome the instability problems in the smart grid. The effectiveness of the proposed control strategy is proved by comparing the results with PID controller results. The transient performance of smart grid is measured by the famous power quality indices (total harmonic distortion in voltage and current, voltage sag, and voltage swell).

The modified IEEE 5-bus system connected with wind turbine installed at bus 3, non-linear loads near to DG and SMES controlled by MPC is used to judge the performance of the SMES with the proposed MPC controller strategy, the implementation is done using MATLAB\Simulink the implemented micro-grid system model. The system is analysed in three cases, namely no storage devices, BESS and SMES controlled by PID controller, and BESS and SMES controlled by MPC controller in order to prove the effectiveness of SMES over BESS and prove the effectiveness of MPC control strategy over PID control strategy in damping oscillation in the grid and improve transients as well as the dynamic stability of power system.

The rest of this paper is organised as follows: Section 2 covers the different types of energy storage devices. Model of VSC-based SMES system will be discussed in Section 3. However, Section 4 illustrates the problem formulation and the proposed technique in Section 5, followed by computer results and simulations as in Section 6. Finally, the conclusion will be drawn in Section 7.

2 Types of energy storage devices

The increasing focus on large-scale integration of renewable energy sources (wind turbine and photovoltaic system) introduces

Table 1 Comparison between different types of energy storage systems

Type	Energy density, Wh/kg	Energy efficiency, %	Power density, W/kg	Response time	Environmental effect
BESS	25–250	60–90	100–3000	milliseconds	toxic
supercapacitors	<50	95	4000	milliseconds	benign
flywheel	100–130	95	1000	instantaneous	benign
CAES	10–30	50	fair	seconds–minutes	benign
PHS	0.3	65–80	fair	seconds–minutes	benign
SMES	30–80	95	very high	instantaneous	benign

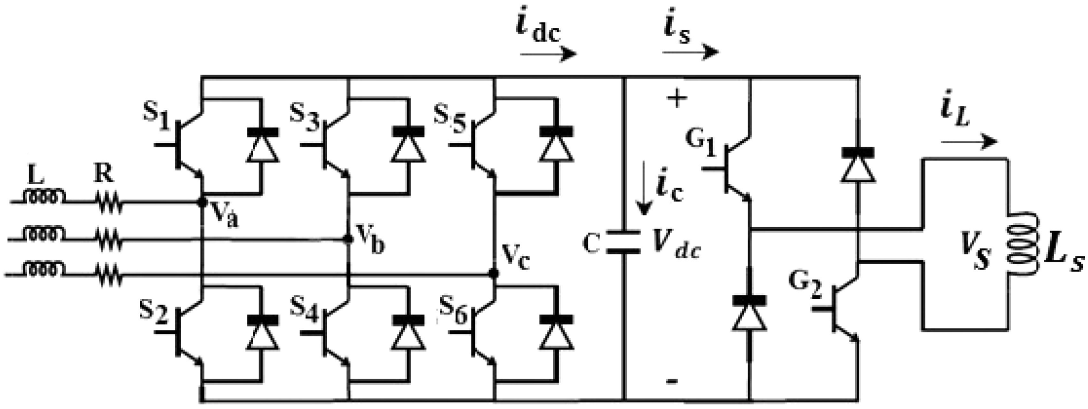

Fig. 1 *Main circuit of VSC-based SMES*

the need for energy storage in order to damp the fluctuations in power system. Energy storage system can be classified as follows:

- *BESS*: It stores energy chemically and uses electrochemical reactions to produce electricity at a fixed voltage [7]. The advantages of BESS are its convenient size and convenient voltage characteristics. However, it has a short life cycle. Moreover, it contains hazardous chemicals.
- *Supercapacitor*: It is a high-capacity electrochemical capacitor with capacitance values much higher than other capacitors. However, it has lower-voltage limits [8].
- *Flywheel energy storage*: It stores energy in the form of momentum in a rotating wheel or cylinder [9]. It has a high-power density and a long life cycle. However, it has large standby losses, low-energy density, and potentially dangerous failure modes.
- *Compressed air energy storage (CAES)*: In which air is compressed and stored in large underground spaces. Then, it is used in gas turbine generators [10]. Although it has a huge power capacity, it requires special locations, expensive initial, and maintenance cost and it has slow start.
- *PHS*: It is a type of hydroelectrical energy storage [11]. It stores energy in the form of gravitational potential energy of water and during the periods of high electrical demand, the stored water is released through turbines to produce electrical power. Although it is pollution free, it is expensive and once it is used it cannot be reused until the water is pumped again.
- *Super magnetic energy storage (SMES)*: It stores energy in the magnetic field produced by current flowing through a superconducting coil [4]. SMES has been used as a large-scale technology because it offers many advantages such as instantaneous energy discharge and it has a high storage efficiency that exceeds 97%. Moreover, SMES contains no dangerous chemicals. In addition, theoretically, it has an infinite number of recharge cycles. However, it has a high cost due to the cryogenic system that must be used to keep the superconducting coil within the superconducting state.

To conclude, a comparison between different types of energy storage systems is listed in Table 1 [12].

According to SMES topology configuration [13], there are three kinds of power conducting system (PCS) for SMES: (i) thyristor-based PCS that can control active power mainly. However, it has a little effect on controlling the reactive power. (ii) VSC-based PCS that can control active and reactive powers independently. Moreover, it can provide continuous rated volt-Ampere reactive (VAR) capacity. (iii) Current-source converter-based PCS such as (VSC)-based PCS. In this paper, VSC-based SMES is chosen as it controls both active and reactive powers.

Various control strategies have been proposed for the VSC, namely Ivanović *et al.*[14] proposed an improvement of dual vector current control strategies for energy storage devices with needed positive and negative decompositions for voltage and current. Therefore, additional controllers are required to control both positive and negative sequences which made the control more complex. A PI controller was used for the current controller as proposed by Li *et al.* [15]. Despite that, under unbalanced voltage condition, PI controller was not able to suppress the harmonics. Zeng and Chang [16] proposed VSC control based on a combination between space vector modulation and predictive control which provides constant switching frequency. Furthermore, this system had some issues related to the parameter sensitivity and control delays. However, the MPC is the most promising controller that is generally intended to deal with complex, dynamic, and non-linear systems. MPC predicts the behaviour of VSC-based SMES and damps any harmonics [17].

3 Model of VSC-based SMES system

VSC-based SMES (as shown in Fig. 1) consists of two main parts: the first is the coil that has been cooled to <9.8 K using liquid helium that brings the temperature down to 4.2 K, in order to reach the superconducting state which means that ohmic losses nearly equal to zero. The second part is the power conversion system (PCS) which consists of VSC and dc–dc chopper.

The VSC is used to control active and reactive powers taking into consideration system needs. On the other hand, dc–dc chopper is used to control current flowing through the superconducting coil.

A magnetic field is created by the flow of direct current through the superconducting coil and the current is circulated indefinitely with almost zero loss, so the energy remains stored in the form of a magnetic field for a long time. This stored energy can be released back to the electrical power system by converting the magnetic energy stored in it to electrical energy.

To emphasise the stability of the renewable energy resource (wind turbine system), the SMES unit is installed at point of common coupling (PCC) between renewable resources and the grid. The superconductive coil is charged/discharged according to the grid needs. The superconductive coil stores energy without any losses. Furthermore, if there is any power deficiency in the grid SMES discharges its stored energy to the grid. Otherwise, SMES is in the charging mode and absorbs the excess energy from the power system. The SMES finishes charging when the power system returns to its steady state [18]. The SMES changes its status to charge, discharge, or keeps its stored energy depending on the dc–dc chopper mode. The voltage vector of a dc–dc chopper is determined by the gating signals G_1, G_2 [19].

As shown from Table 2 when G_1 and G_2 are 0 s, the SMES works in discharging mode and injects power into the grid. On the other hand, when G_1 and G_2 are 1 s, the SMES is in charging mode. Otherwise, the dc current continually circulates in both dc–dc chopper and the superconducting coil without any losses which are called standby mode or freewheeling mode. The VSC provides a power electronic interface between the ac power system and the superconducting coil.

4 Problem formulation

VSC-based SMES consists of two-level VSC and dc–dc chopper. The MPC is proposed to control both converters. Under unbalanced voltage condition, the VSC current has two components: positive and negative sequences. So, the reference values of grid current in the stationary coordinates $i_{\alpha,\mathrm{ref}}$, $i_{\beta,\mathrm{ref}}$ are calculated as summation of positive and negative sequence components

$$i_{\alpha,\mathrm{ref}} = i^{\mathrm{p}}_{\alpha,\mathrm{ref}} + i^{\mathrm{n}}_{\alpha,\mathrm{ref}} \tag{1}$$

$$i_{\beta,\mathrm{ref}} = i^{\mathrm{p}}_{\beta,\mathrm{ref}} + i^{\mathrm{n}}_{\beta,\mathrm{ref}} \tag{2}$$

where $i^{\mathrm{p}}_{\alpha,\mathrm{ref}}$ is a reference value of the positive sequence component of grid current in the stationary coordinate α, $i^{\mathrm{n}}_{\alpha,\mathrm{ref}}$ is a reference value of the negative sequence component of grid current in the stationary coordinate α, $i^{\mathrm{p}}_{\beta,\mathrm{ref}}$ is a reference value of the positive sequence component of grid current in the stationary coordinate β, and $i^{\mathrm{n}}_{\beta,\mathrm{ref}}$ is a reference value of the negative sequence component of grid current in the stationary coordinate β.

According to the mathematical model, the reference grid current in the stationary coordinate ($i_{\alpha\beta}$) is a function of ac-side voltage in the stationary coordinate ($e_{\alpha\beta}$). Therefore, it is determined as follows [20]:

$$\begin{bmatrix} i^{\mathrm{p}}_{\alpha,\mathrm{ref}} \\ i^{\mathrm{p}}_{\beta,\mathrm{ref}} \end{bmatrix} = \begin{bmatrix} m & n \\ -n & m \end{bmatrix} \begin{bmatrix} e^{\mathrm{p}}_{\alpha} \\ e^{\mathrm{p}}_{\beta} \end{bmatrix} \tag{3}$$

$$\begin{bmatrix} i^{\mathrm{n}}_{\alpha,\mathrm{ref}} \\ i^{\mathrm{n}}_{\beta,\mathrm{ref}} \end{bmatrix} = \begin{bmatrix} m & n \\ -n & m \end{bmatrix} \begin{bmatrix} e^{\mathrm{n}}_{\alpha} \\ e^{\mathrm{n}}_{\beta} \end{bmatrix} \tag{4}$$

where e^{p}_{α} is a value of the positive sequence component of the grid voltage in the stationary coordinate α, e^{n}_{α} is a value of the negative sequence component of the grid voltage in the stationary coordinate α, e^{p}_{β} is a value of the positive sequence component of the grid voltage in the stationary coordinate β, and e^{n}_{β} is a value of the negative sequence component of the grid voltage in the stationary coordinate β.

Table 2 Voltage vector of dc–dc chopper

G_1	G_2	$\boldsymbol{V}_{\mathrm{s}}$
0	0	$-V_{\mathrm{dc}}$
0	1	0
1	0	0
1	1	V_{dc}

The coefficient m is the active power of dc-side provided by the three-phase VSC

$$m = \frac{2P_{\mathrm{av,ref}}}{3\left[(e^{\mathrm{p}}_{\alpha})^2 + (e^{\mathrm{p}}_{\beta})^2 - (e^{\mathrm{n}}_{\alpha})^2 - (e^{\mathrm{n}}_{\beta})^2\right]} \tag{5}$$

$$n = \left(1 - \sqrt{1 - 4(\omega L m)^2}/(2\omega L)\right) \tag{6}$$

Moreover, $\omega = 2\pi f$, $f = 50$ Hz.

According to (3) and (4), the reference of current has two sequence components under unbalanced voltage condition, the first part is related to the coefficient m, where m is a function of the active power of dc-side provided by the three-phase VSC. By controlling this part, a stable active power in ac-side can be obtained and voltage ripple is eliminated. The second part depends on the coefficient n, where n is a function of the ac-side inductance which represents the disturbance component for ac-side power. The influence of the ac-side inductance on ac-side power can be eliminated by manipulating this part.

5 Proposed technique

Model predictive control (MPC) is a control strategy that is based on numerical optimisation, at each interval a future control inputs and future plant output are predicted and optimised using MPC model.

MPC can be used to control VSC with rapid and dynamic performance suitable with the electrical grid behaviour. The MPC used as a current controller for VSC, with high performance and no static error under unbalanced voltage condition.

The MPC is used to predict the grid-side current in every sampling period to achieve the optimum reference current according to the historical data of the grid. Then, MPC determines the optimum switch states of the VSC-insulated gate bipolar transistor. The prediction of the grid-side current at next instant in MPC can be obtained through the following equations [20]:

$$i_{\alpha}(k+1) = \left(1 - \frac{RT_{\mathrm{s}}}{L}\right) i_{\alpha}(k) + \frac{T_{\mathrm{s}}}{L}(V_{\alpha}(k) - v_{\alpha}(k)) \tag{7}$$

$$i_{\beta}(k+1) = \left(1 - \frac{RT_{\mathrm{s}}}{L}\right) i_{\beta}(k) + \frac{T_{\mathrm{s}}}{L}\left(V_{\beta}(k) - v_{\beta}(k)\right) \tag{8}$$

where T_{s} is the sampling period of a controller, and $\boldsymbol{V}_{\alpha}$, $\boldsymbol{V}_{\beta}$ are the possible voltage vectors at time k, and v_{α}, v_{β} are the three-phase grid voltages at time k.

The dynamic current of the SMES coil can be represented in the discrete time model as follows:

$$i^{\mathrm{p}}_{L}(k+1) = \boldsymbol{i}_{L}(k) + \left(\frac{T_{\mathrm{s}}}{L_{\mathrm{s}}}\right)(\boldsymbol{V}_{\mathrm{s}}(k)) \tag{9}$$

where $\boldsymbol{L}_{\mathrm{s}}$ is the inductance of the SMES coil, $\boldsymbol{i}_{L}(k)$ is the current of the SMES coil at time k, and $\boldsymbol{V}_{\mathrm{s}}(k)$ is the possible voltage vector of the dc–dc chopper at time k.

The predicted current for the dc–dc chopper can be calculated using the following equation:

$$i_{\mathrm{s}}(k+1) = G_1\, i_l(k+1) \tag{10}$$

where $i_{\mathrm{s}}(k+1)$ is a predicted current dc–dc chopper at time $k+1$, $\boldsymbol{G}_1$ is the switching states of the dc–dc chopper, and $i_l(k+1)$ is a predicted current of SMES coil at time $(k+1)$.

The predicted capacitor voltage at time $(k+1)$ can be calculated as follows:

$$u_{\mathrm{C}}(k+1) = i_{\mathrm{C}}(k) \cdot T_{\mathrm{s}}/C + V_{\mathrm{dc}}(k) \tag{11}$$

where $u_{\mathrm{C}}(k+1)$ is the predicted capacitor voltage at time $k+1$, $i_{\mathrm{C}}(k)$ is the measured capacitor current at time k, $V_{\mathrm{dc}}(k)$ is the

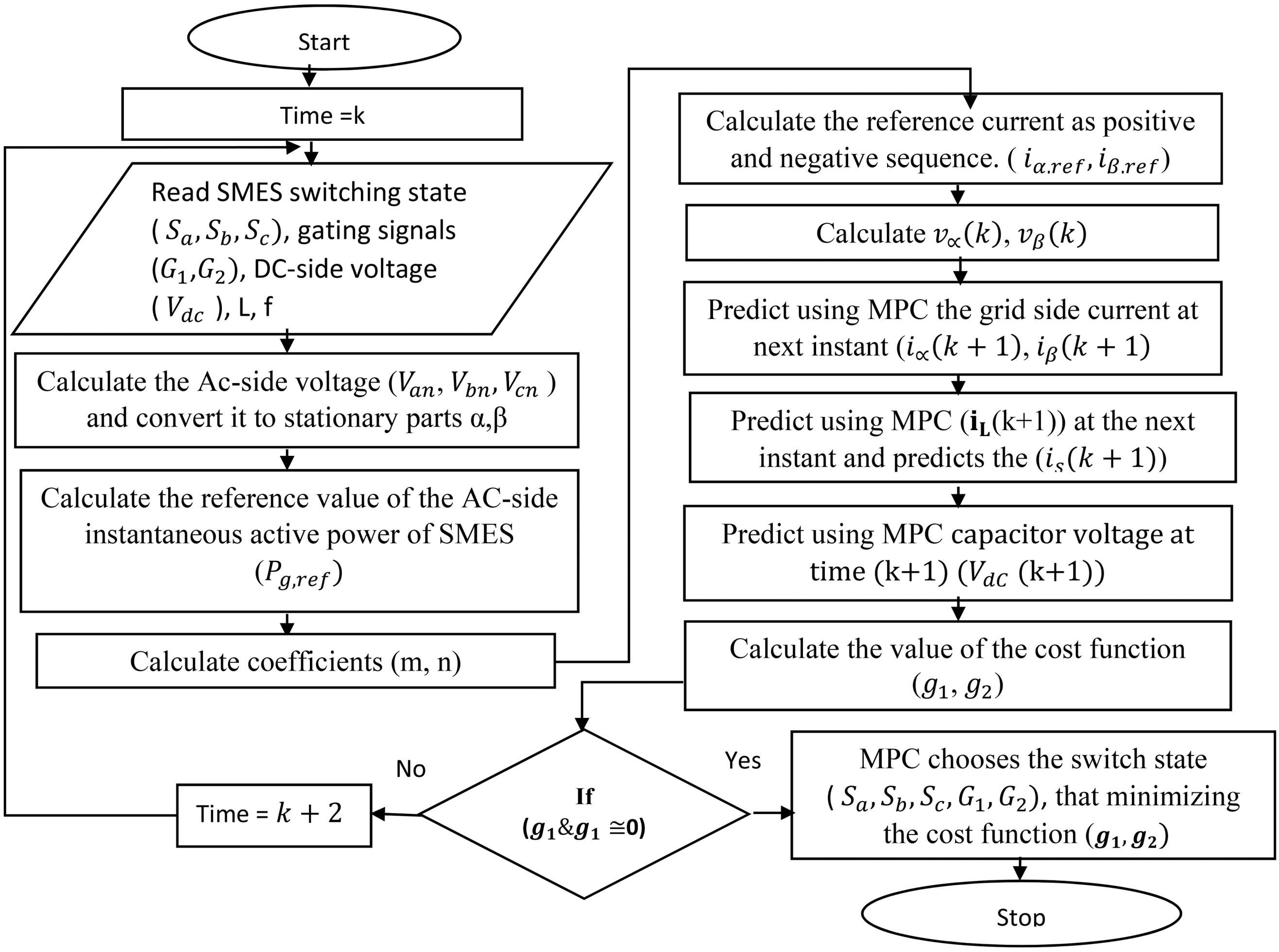

Fig. 2 *Flowchart for the proposed strategy*

measured capacitor voltage at time k, and C is the capacity of the capacitor.

The MPC evaluates the predictive value of the grid-side current in each instant under each switch states to minimise the VSC and dc–dc chopper switching state. The MPC repeats the above procedure until it satisfies the cost function g_1

$$g_1 = |i_{\alpha,\,\mathrm{ref}}(k+2) - i_\alpha(k+2)| + |i_{\beta,\,\mathrm{ref}}(k+2) - i_\beta(k+2)| \qquad (12)$$

The cost function g_2 represents the difference between the reference value of dc-side voltage of VSC-based SMES and the predicted dc-side voltage at time $(k+1)$

$$g_2 = u_{\mathrm{c,\,ref}} - u_{\mathrm{c}}(k+1) \qquad (13)$$

The MPC flowchart for the proposed strategy in this paper is shown in Fig. 2.

6 Computer results and simulation

To verify the effectiveness of the proposed MPC controller and the merits of SMES, IEEE 5-bus system is chosen as the benchmark. IEEE 5-bus system is connected with non-linear loads and DG (wind turbine) as shown in Fig. 3.

The comparative study is done in terms of most well-known power quality indices metrics [21]. The performance metrics used are voltage sag and voltage swell:

- *Voltage dips (sags)* is a short duration reduction in root-mean-square (RMS) voltage which can be caused by a short circuit, overload, or starting of electric motors. A voltage sag occurs when the RMS voltage decreases between 10 and 90% of nominal voltage for the one-half cycle to 1 min.
- *Voltage swells* is an increase in the RMS of the supply voltage to a value between 110 and 180% of the declared voltage, followed by a voltage recovery after a short period of time.

BESS and SMES specifications are shown in Tables 3 and 4. Moreover, VSC specifications are shown in Table 5.

6.1 IEEE 5-bus system with SMES-/BESS-based PID controller

To study the performance of the SMES/BESS with PID controller, a scenario has been assumed that wind turbine system is installed at bus 3 with variant wind speed which causes a fluctuation in its output power as shown in Fig. 4, and it is connected with non-linear loads that have a large current disturbance as shown in Fig. 5.

Storage system with PID controller is installed at PCC and connected with the grid at 0.3 s. Then modified IEEE 5-bus is tested with SMES with PID controller and with BESS with PID controller at the same grid conditions. Results are measured at wind turbine bus as follows.

Bus 3 (wind turbine bus): It is the most fluctuation bus and it is the PCC, so it is the most suitable bus to measure the performance of storage system (SMES/BESS) with (PID/MPC) controller in enhancing system stability:

I. *Voltage at bus 3 (wind turbine bus):* The waveform of the voltage at bus 3 (wind bus) is shown in Fig. 6, when BESS-based PID controller is connected to the grid at 0.3 s. From 0 to 0.3 period time before storage device is connected to the grid, the grid has a variation between the three phases of voltage that result from a wind turbine and non-linear loads. When BESS-based PID connected to the grid at 0.3 s, BESS is tried to dampen fluctuation

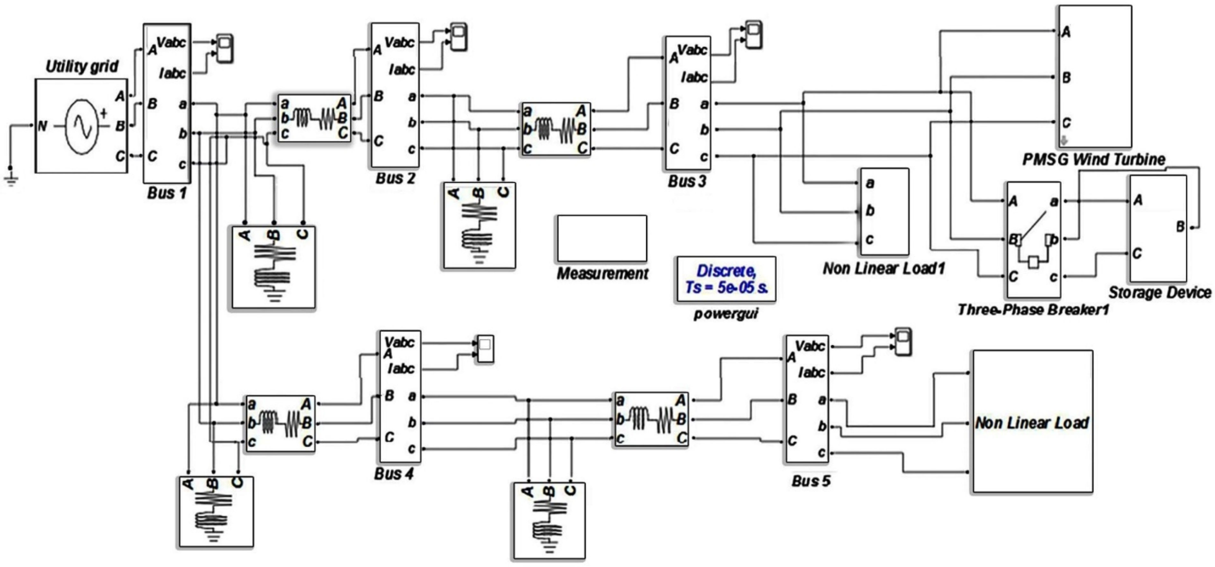

Fig. 3 *Modified IEEE 5-bus system*

Table 3 BESS specifications

energy capacity	1 MJ
battery voltage	760–1050 V_{dc}
battery current	1316 A_{dc}
output voltage	22.9 kV
output current	1312 A

Table 4 SMES specifications

energy capacity	1 MJ
inductance	8 H
rated current	0.45 kA
dc-link capacitor	10 μF
peak voltage	20 kV

in voltage. However, it causes instability between the three phases of voltage.

Fig. 7 shows that the voltage at wind turbine bus using SMES-based PID controller which is connected with the grid at time = 0.3 s. It is cleared that the storage system suppressing fluctuation in voltage waveform. Moreover, it is succeeded to improve voltage stability between the three phases of voltage.

It is revealed from the figures that SMES with PID controller succeeded to suppress fluctuation between three phases. Moreover, it maintains stability between the three phases of the voltage at its rated value 1 pu.

Table 5 VSC specifications

rated power	1 MVA
dc voltage	50 kV
|ac voltage	24.5 kV_{rms}
peak voltage	20 kV
filter impedance ($r + j\omega L$)	(0.01 + j0.25) pu

Table 6 shows the behaviour of the three phases of voltage in two period time. The first period is from 0 to 0.3 s before the storage devices are connected to the grid. The second period is from 0.3 to 0.5 s when the storage device SMES-/BESS-based PID controller are connected to the grid.

It is evident from Table 6 that SMES-based PID successes in release voltage sag. Moreover, it dampens voltage swell in phase A and phase B and it reduces voltage swell in phase C from 0.8 to 0.35 pu. On the other hand, BESS-based PID causes voltage sag in phase A equal to 0.2 pu. Furthermore, it releases the voltage swell in phase B and dampens the voltage swell in phase C from 0.8 to 0.45 pu. Therefore, SMES-based PID has the better performance in releasing system disturbance and enhancing voltage stability between the three phases.

II. *Active power at wind turbine bus*: The active power in per unit (pu) at wind turbine bus calculated by storage device SMES/BESS controlled by PID controller is shown in Fig. 8.

It is revealed from Fig. 8 that in period (0–0.3) s before a storage device connected to the grid, the system has a disturbance in active power waveform. However, at 0.3 s when SMES-/BESS-based PID connected to the grid, the storage devices increase active

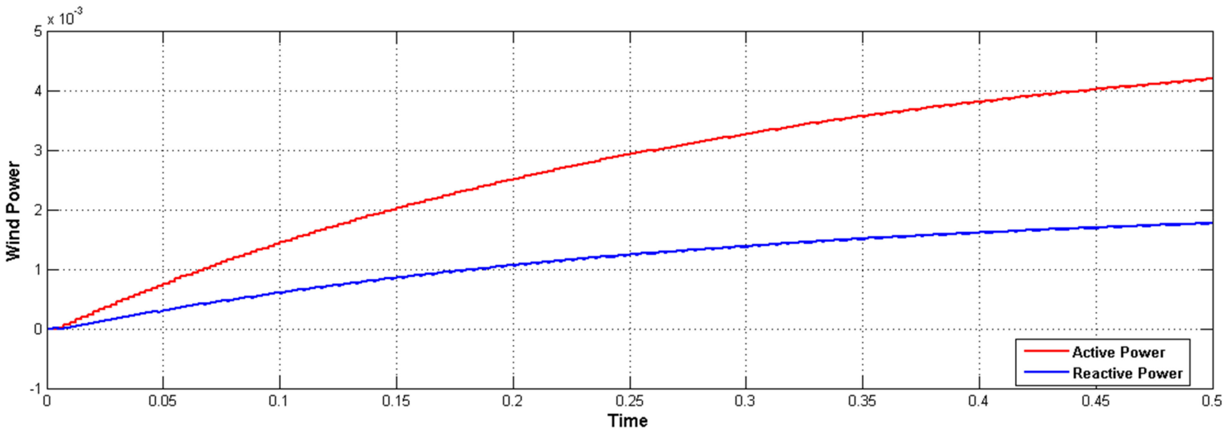

Fig. 4 *Wind turbine power in pu*

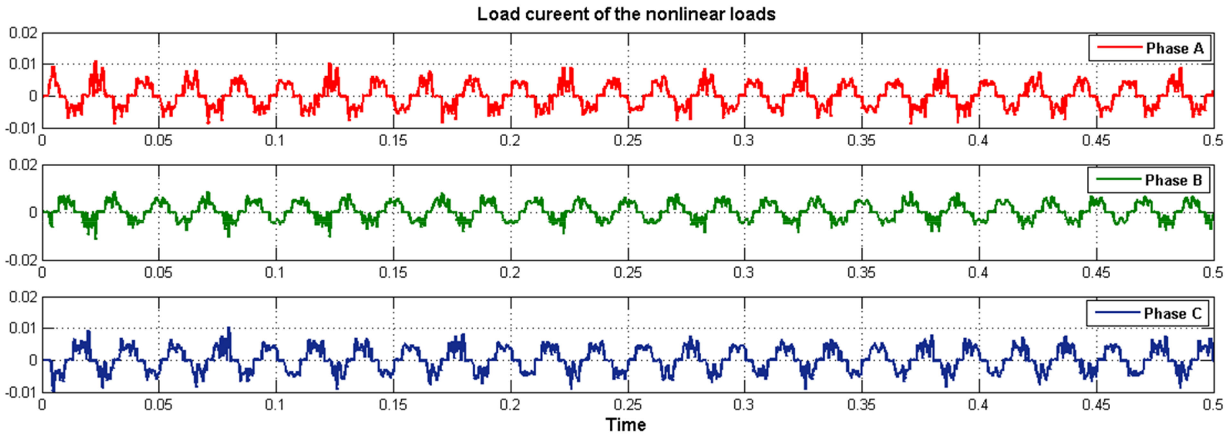

Fig. 5 *Load current of the non-linear loads in pu*

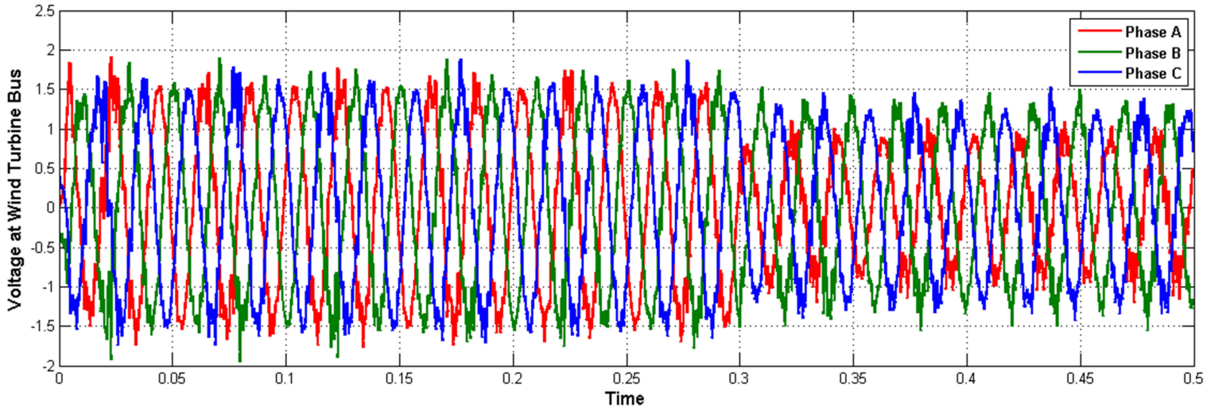

Fig. 6 *Voltage measurement in pu at wind turbine bus with BESS-based PID control*

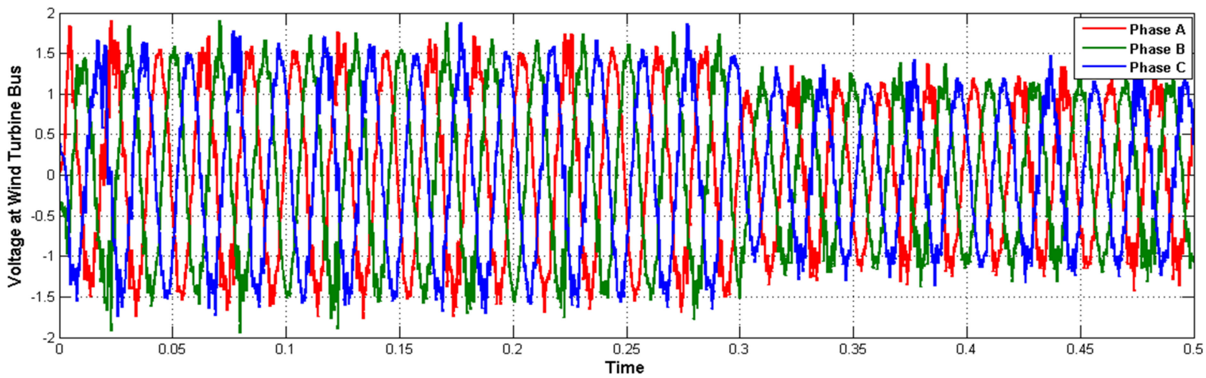

Fig. 7 *Voltage measurement in pu at wind turbine bus with SMES-based PID control*

Table 6 Voltage sag/swell at wind turbine bus with/without storage devices based PID

With/without storage-based PID	Without (0–0.3) s	BESS (0.3–0.5) s	SMES (0.3–0.5) s
voltage sag, pu	no	0.2 (phase A)	no
voltage swell, pu	0.8 (phases A, B, and C)	0.45 (phase C)	0.35 (phase C)

power in order to suppress disturbance in voltage and current. Maximum overshoot (M_P), which is the maximum peak value of the response curve and indicates the relative stability of the system. It can be used to compare between SMES-/BESS-based PID. BESS-based PID has M_P equal to 18.42%, that is, greater than SMES-based PID overshoot (M_P) which is equal to 10.52%.

III. *Reactive power at wind turbine bus:* Reactive power in pu at wind turbine bus to get voltage balanced and at its desired value as shown in Fig. 9.

From Fig. 9, storage device SMES-/BESS-based PID controller inject reactive power into the grid in order to suppress fluctuation in voltage and current. It is evident from this figure that BESS has an overshoot (M_P) that refers to an output exceeding its final steady-state value equal to 6.25% which is greater than SMES overshoot (M_P) that is equal to 4.375%.

6.2 IEEE 5-bus system with SMES-/BESS-based MPC controller

I. *Voltage at bus 3(wind turbine bus):* Fig. 10 shows the voltage waveform at wind turbine bus when storage device SMES-/BESS-based MPC controller is connected to the grid at time 0.3 s.

As shown from Fig. 10 that storage device SMES-/BESS-based MPC suppressed the fluctuation in voltage with the same amplitude. MPC controller successes to make SMES and BESS give the same performance at the same grid conditions.

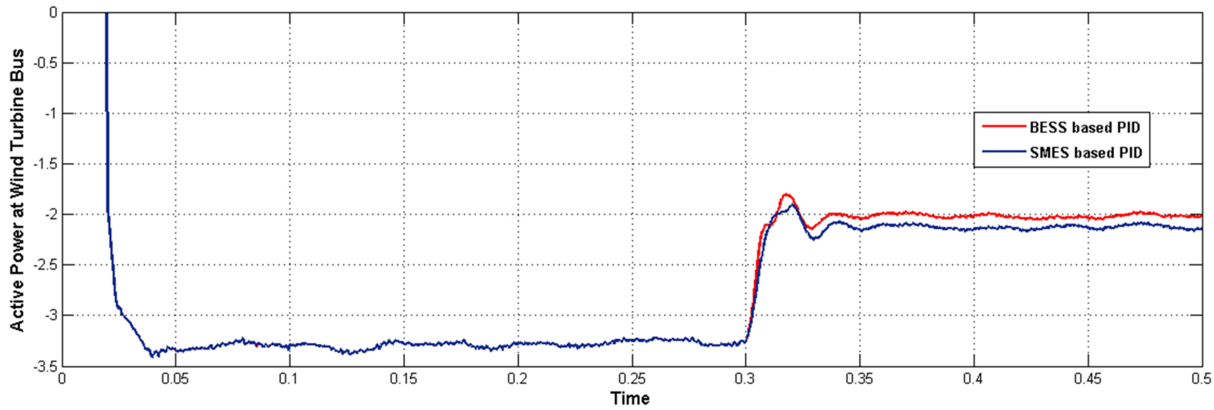

Fig. 8 *Active power in pu at wind turbine bus with SMES-/BESS-based PID controller*

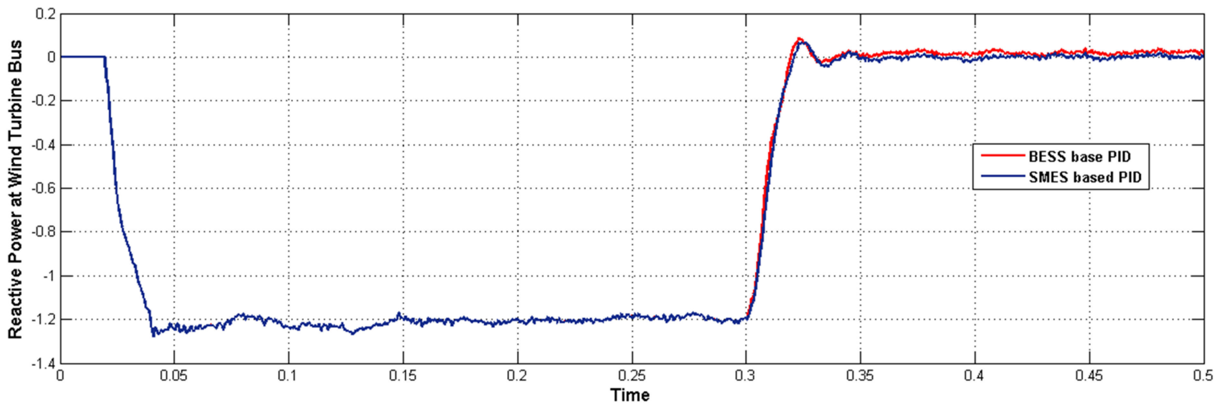

Fig. 9 *Reactive power in pu at wind turbine bus with SMES-/BESS-based PID controller*

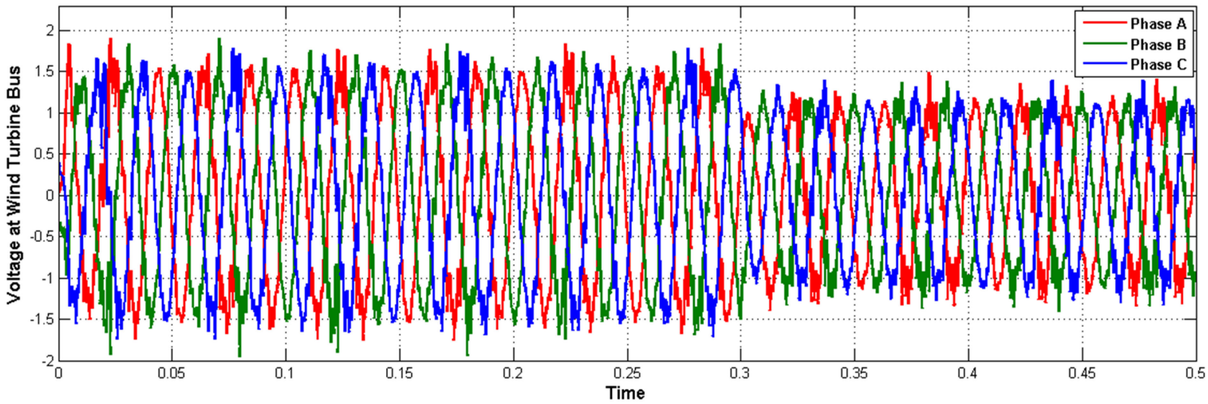

Fig. 10 *Voltage measurement in pu at wind turbine bus with SMES-/BESS-based MPC control*

Table 7 Voltage sag/swell at wind turbine bus storage devices based MPC

With/without storage-based MPC	Without (0–0.3) s	BESS/SMES (0.3–0.5) s
voltage sag, pu	no	no
voltage swell, pu	0.8 (phases A, B, and C)	0.5 (phase A)

Table 7 shows the behaviour of the grid before and after connected with the storage device SMES-/BESS-based MPC.

As illustrated in Table 7 that before storage device is connected to the grid in the period (0–0.3) s when a voltage swell problem occurs in the three phases of voltage, which causes an instability problem. On the other hand, when (BESS/SMES)-based MPC connected with the grid at 0.3 s the two storage devices get the same performance. They succeeded to suppress voltage swell in phase B and phase C and dampen voltage swell in phase A from 0.8 to 0.5 pu.

II. *Active power at wind turbine bus*: Active power in pu at wind turbine is measured in the two cases with storage device SMES-/BESS-based MPC control strategy and is monitored at Fig. 11.

At period (0–0.3) s, when the load varies and the system has no storage devices, there is a drop in active power of the grid and a disturbance in voltage waveform as shown in Fig. 11. When the storage device SMES-/BESS-based MPC control connected with the grid at 0.3 s, they inject active power to the grid in order to suppress any harmonics in voltage waveform. As shown from Fig. 11 that MPC control enhancing the performance of BESS to nearly equal the performance of SMES. Moreover, SMES-/BESS-based MPC have the same overshoot (M_P) which is equal to 10.52%.

III. *Reactive power at wind turbine bus*: Reactive power in pu at wind turbine bus with and without any storage device-based MPC

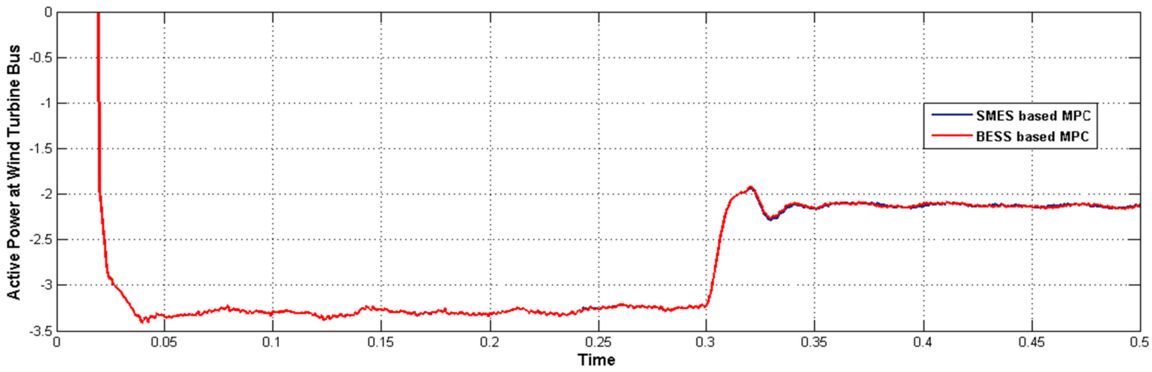

Fig. 11 *Active power in pu at wind turbine bus with SMES-/BESS-based MPC controller*

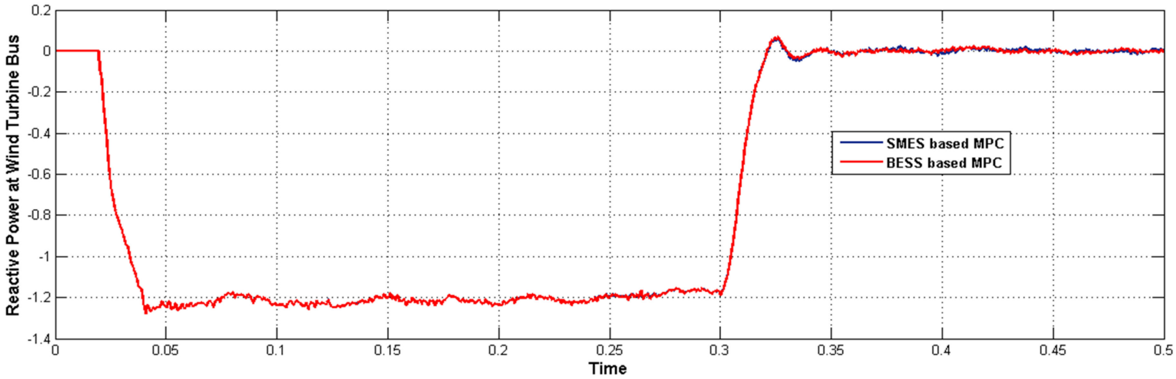

Fig. 12 *Reactive power in pu at wind turbine bus with SMES-/BESS-based MPC controller*

control strategy in order to enhance voltage waveform is shown in Fig. 12.

As shown in Fig. 12 at period (0–0.3) s, the system is without any storage devices and there is a disturbance in reactive power waveform results from non-linear loads and variation in wind turbine output power. However, when a storage device SMES-/BESS-based MPC control strategy is connected to the grid to dampen the fluctuation in voltage, they injected the same reactive power to the grid with the same maximum overshoot equal to (M_P) 4.375%, which means that MPC strategy improves the performance of BESS to equalise the performance of SMES.

7 Conclusion

This paper proposed a new MPC-based control strategy for (BESS/SMES) storage devices to enhance the transient performance of smart grid with wind power penetration. To prove the effectiveness of the proposed control strategy, a comparison between system performance of the MPC controller and the PID controller is held in different situations. A modified IEEE 5-bus system is simulated using MATLAB/Simulink with SMES with (PID/MPC) controller and with BESS with (PID/MPC) controller at the same grid conditions. As shown from the results, the proposed MPC control strategy enhances the transient performance of the smart grid with both storage devices (BESS/SMES). Also, the results of the simulation demonstrate that the SMES is a fast response storage device that can suppress the performance fluctuation in the smart grid system and enhance smart grid stability with both controls (PID/MPC). So, in this case, a PID control is fair enough. On the other hand, when using the BESS storage device, the performance of the system when using the proposed MPC control is much better than using PID controller as the battery is a slow storage device. So, using MPC controller is required to dampen any disturbance in the smart grid.

8 References

[1] Zhang, S., Huang, M.: 'Microgrid: a strategy to develop distributed renewable energy resource'. Proc. Int. Conf. Electrical and Control Engineering (ICECE), Yichang, 2011, pp. 3520–3523

[2] Ribeiro, P.F., Johnson, B.K., Crow, M.L., *et al.*: 'Energy storage systems for advanced power applications', *Proc. IEEE*, 2001, **89**, (12), pp. 1744–1756

[3] Xie, Y., Song, M., Shi, J., *et al.*: 'Simulation on a micro-grid system based on superconducting magnetic energy storage'. Int. Power Electronics and Application Conf. and Exposition, Shanghai, 2014, pp. 1451–1455

[4] Chen, X.Y., Jin, J.X., Xin, Y.: 'Integrated SMES technology for modern power system and future smart grid', *IEEE Trans. Appl. Supercond.*, 2014, **24**, (5), pp. 1–5

[5] Mundackal, J., Varghese, A.C., Sreekala, P., *et al.*: 'Grid power quality improvement and battery energy storage in wind energy systems'. 2013 Annual Int. Conf. Emerging Research Areas and 2013 Int. Conf. Microelectronics, Communications and Renewable Energy (AICERA/ICMiCR), Kanjirapally, 2013, pp. 1–6

[6] Rau, M., Schroder, D.: 'Model predictive control with nonlinear state space models'. Seventh Int. Workshop Advanced Motion Control, 2002, 2002, pp. 136–141

[7] Xia, T., Li, M., Zi, P., *et al.*: 'Modeling and simulation of battery energy storage system (BESS) used in power system'. 2015 Fifth Int. Conf. Electric Utility Deregulation and Restructuring and Power Technologies (DRPT), Changsha, 2015, pp. 2120–2125

[8] Wang, J., Zhang, J., Zhong, Y.: 'Study on a super capacitor energy storage system for improving the operating stability of distributed generation system'. Third Int. Conf. Electric Utility Deregulation and Restructuring and Power Technologies, 2008, DRPT 2008, Nanjuing, 2008, pp. 2702–2706

[9] Wu, J., Wen, J., Sun, H.: 'A new energy storage system based on flywheel'. Power & Energy Society General Meeting, 2009, PES 09, Calgary, AB, 2009

[10] Martínez, M., Molina, M.G., Mercado, P.E.: 'Dynamic performance of compressed air energy storage (CAES) plant for applications in power systems'. 2010 IEEE/PES Transmission and Distribution Conf. and Exposition: Latin America (T&D-LA), Sao Paulo, 2010, pp. 496–503

[11] Raudsaar, U., Drovtar, I., Rosin, A.: 'Overview – pumped-hydro energy storage for balancing wind energy forecast errors'. 2014 Electric Power Quality and Supply Reliability Conf. (PQ), Rakvere, 2014, pp. 133–138

[12] Biswas, M., Azim, M., Saha, T., *et al.*: 'Towards implementation of smart grid: an updated review on electrical energy storage systems', *Smart Grid Renew. Energy*, 2013, **4**, (1), pp. 122–132

[13] Ali, M.H., Wu, B., Dougal, R.A.: 'An overview of SMES applications in power and energy systems', *IEEE Trans. Sustain. Energy*, 2010, **1**, (1), pp. 38–47

[14] Ivanović, Z.R., Adžić, E.M., Vekić, M.S., *et al.*: 'HIL evaluation of power flow control strategies for energy storage connected to smart grid under unbalanced conditions', *IEEE Trans. Power Electron.*, 2012, **27**, (11), pp. 4699–4710

[15] Li, S., Haskew, T.A., Xu, L.: 'Control of HVDC light system using conventional and direct current vector control approaches', *IEEE Trans. Power Electron.*, 2010, **25**, (12), pp. 3106–3118

[16] Zeng, Q., Chang, L.: 'An advanced SVPWM-based predictive current controller for three-phase inverters in distributed generation systems', *IEEE Trans. Ind. Electron.*, 2008, **55**, (3), pp. 1235–1246

[17] Padimiti, D.S., Chowdhury, B.H.: 'Superconducting magnetic energy storage system (SMES) for improved dynamic system performance'. Proc. IEEE Power Engineering Society General Meeting, June 2007, pp. 1–6

[18] Nielsen, K.E., Molinas, M.: 'Superconducting magnetic energy storage (SMES) in power systems with renewable energy sources'. 2010 IEEE Int. Symp. Industrial Electronics, Bari, 2010, pp. 2487–2492

[19] Nguyen, T.T., Yoo, H.J., Kim, H.M.: 'Applying model predictive control to SMES system in microgrids for eddy current losses reduction', *IEEE Trans. Appl. Supercond.*, 2016, **26**, (4), pp. 1–5

[20] Zhou, Z., Xia, C., Gu, X., *et al.*: 'Model predictive control of three-phase voltage source rectifiers under unbalanced grid voltage conditions'. Seventh IET Int. Conf. Power Electronics, Machines and Drives (PEMD 2014), Manchester, 2014, pp. 1–6

[21] Caramia, P., Carpinelli, G., Verde, P.: 'Power quality indices in liberalized markets', 2009